

# Pattern electroretinogram association with spectral domain-OCT structural measurements in glaucoma

C Bowd, A Tafreshi, LM Zangwill, FA Medeiros, PA Sample and RN Weinreb

## Abstract

**Purpose** To describe the association between pattern electroretinogram (PERG) amplitude and spectral domain-optical coherence tomography (SD-OCT) macular thickness, retinal nerve fibre layer (RNFL) thickness and optic disc topography measurements.

**Subjects and methods** Both eyes ( $n = 132$ ) of 66 glaucoma patients (mean age = 67.9 years) enrolled in the University of California, San Diego, CA, USA, Diagnostic Innovations in Glaucoma Study (DIGS) were included. Eyes were tested with PERG (Glaide PERGLA, Lace Elettronica, Pisa, Italy), RTVue SD-OCT (Optovue Inc., Fremont, CA, USA) GCC, and NHM4 protocols on the same day. Of the 66 enrolled patients, 43 had glaucoma defined by repeated abnormal standard automated perimetry (SAP) results in at least one eye and 23 were glaucoma suspects defined by a glaucomatous-appearing optic disc by physicians' examination in at least one eye and normal SAP results in both eyes.

**Associations ( $R^2$ ) were determined between PERG amplitude ( $\mu\text{V}$ ) and SD-OCT macular ganglion cell complex (GCC) thickness ( $\mu\text{m}$ ), macular thickness ( $\mu\text{m}$ ), macular outer retinal thickness (macular thickness minus GCC thickness) ( $\mu\text{m}$ ), RNFL thickness ( $\mu\text{m}$ ), neuroretinal rim area ( $\text{mm}^2$ ), and rim volume ( $\text{mm}^3$ ).**

**Results** PERG amplitude was significantly associated with GCC thickness ( $R^2 = 0.179$ ,  $P < 0.001$ ), RNFL thickness ( $R^2 = 0.174$ ,  $P < 0.001$ ), and macular thickness ( $R^2 = 0.095$ ,  $P < 0.001$ ).  $R^2$  associations with other parameters were not significant (all  $P > 0.624$ ). Significant associations remained for GCC and

average RNFL thickness when age and intraocular pressure at the time of testing were included in multivariate models (both  $P \leq 0.030$ ).

**Conclusions** PERG amplitude is significantly (but weakly) associated with macular GCC thickness, RNFL thickness, and macular thickness. The lack of association between PERG amplitude and macular outer retinal thickness supports previous results, possibly suggesting that the PERG is driven primarily by retinal ganglion cell (inner retinal) responses.

Eye (2011) 25, 224–232; doi:10.1038/eye.2010.203; published online 24 December 2010

**Keywords:** glaucoma; electrophysiology; pattern electroretinogram; spectral domain; fourier domain; optical coherence tomography

## Introduction

The pattern electroretinogram (PERG) is a mass potential that sums information primarily from the electrical potentials of retinal ganglion cells.<sup>1–5</sup> The PERG stimulus isolates the ganglion cell response by using a reversing (ie, contrast modulated) checkerboard or grating pattern that carries no change in overall luminance over time (space-averaged luminance). If the PERG response is measuring retinal ganglion cell activity, it should be associated with the number of retinal ganglion cells. Because retinal ganglion cell damage is the underlying cause of glaucoma-related decreases in visual sensitivity,<sup>6</sup> the PERG should be useful for detecting and monitoring

Hamilton Glaucoma Center, Department of Ophthalmology, University of California, San Diego, La Jolla, CA, USA

Correspondence: C Bowd, Hamilton Glaucoma Center-178, Department of Ophthalmology, University of California, San Diego, 9500 Gilman Drive, La Jolla, CA, 92037-0946, USA  
 Tel: +1 858 822 4510;  
 Fax: +1 858 822 0615.  
 E-mail: cbowd@glaucoma.ucsd.edu

Received: 8 March 2010  
 Accepted in revised form: 31 August 2010;  
 Published online: 24 December 2010

This work was previously presented at the 2009 annual meeting of the Association for Research in Vision and Ophthalmology, Fort Lauderdale, FL, USA.

this disease, and studies indicate that this is the case (see<sup>7</sup> for a recent review).

Optic disc topography and retinal nerve fibre layer (RNFL) thickness measurements obtained using structural imaging techniques are clinical surrogates for assessing retinal ganglion cell number. Therefore, PERG measurements should be associated with these measurements. Previous studies have reported a significant but modest association between PERG amplitude and neuroretinal rim area measured using confocal scanning laser ophthalmoscopy (CSLO)<sup>8,9</sup> (see also<sup>10</sup>) and RNFL thickness measured using both optical coherence tomography (OCT)<sup>9,11–13</sup> (see also<sup>10,14–17</sup>) and scanning laser polarimetry (SLP).<sup>9</sup> These results suggest that PERG amplitude is at least somewhat representative of ganglion cell count. The generally weak associations reported could be attributable, in part, to the structural measurement chosen to represent ganglion cell count.<sup>18</sup> It is possible that average rim area (previously measured by CSLO) and RNFL thickness (previously measured using OCT) are not ideal surrogates. It also is possible that weak cross-sectional associations between PERG and structural measurements might represent a temporal decorrelation between functional and structural damage.<sup>12</sup>

The current study assesses the strength of associations between PERG amplitude and spectral domain-OCT (SD-OCT)-measured macular ganglion cell complex (GCC) thickness, macular thickness, RNFL thickness, and optic disc topography. Because the PERG relies on a centrally presented stimulus, we hypothesized that PERG amplitude would be most strongly associated with macular parameters, in particular GCC thickness.

## Subjects and methods

### Subjects

In all, 132 eyes of 66 glaucoma patients enrolled in the University of California San Diego, CA, USA, Diagnostic Innovations in Glaucoma Study (DIGS) were included in this study. Eyes had good quality stereo-photography (TRC-SS, Topcon Instruments, Paramus, NJ, USA) of the optic disc and reliable (fixation losses  $\leq 33\%$ , false positives, and false negatives  $\leq 15\%$  with no observable testing artifacts) standard automated perimetry<sup>19</sup> (SAP, Humphrey Field Analyzer II with Swedish Interactive Thresholding Algorithm, Carl Zeiss Meditec, Dublin, CA, USA) testing within 6 months of PERG testing.

Each patient underwent an ophthalmologic evaluation including review of medical history, best-corrected visual acuity testing, slit-lamp biomicroscopy, intraocular pressure (IOP) measurement with Goldmann applanation tonometry, gonioscopy, and a dilated slit

lamp examination. To be included in the study, participants needed a best-corrected acuity better than or equal to 20/40, spherical refraction within  $\pm 5.0D$ , cylinder correction within  $\pm 3.0D$ , and open angles on gonioscopy in both eyes at the time of testing. Eyes with coexisting retinal disease, uveitis, or non-glaucomatous optic neuropathy determined on examination or stereo-photograph assessment were excluded.

For this study, glaucoma patients were individuals recruited from our clinic (ie, being treated or followed for glaucoma or suspicion of glaucoma) with a glaucomatous-appearing optic disc and/or repeatable abnormal SAP result in at least one eye. A glaucomatous-appearing optic disc had marked neuroretinal rim thinning (concentric or focal) and/or diffuse or focal RNFL atrophy based on masked assessment of optic disc stereo-photographs. Two experienced observers conducted masked assessment. In cases of disagreement, a third observer adjudicated the decision. An abnormal SAP result had either pattern SD (PSD) with  $P \leq 5\%$  or a glaucoma hemifield test (GHT) outside normal limits. Of the 66 enrolled patients, 43 had glaucoma defined by repeated abnormal SAP results in at least one eye and 23 were glaucoma suspects defined by a glaucomatous-appearing optic disc by physicians' examination in at least one eye and normal SAP in both eyes.

The average (95% confidence interval (CI)) patient age was 67.9 (65.8, 70.0) years, 37 (54%) patients were female and 58 (88%) were Caucasian. Average IOP at the time of PERGLA recording was 15.8 (14.9, 16.6) mmHg, average SAP MD was  $-1.92$  ( $-1.39$ ,  $-2.45$ ) dB, and average SAP PSD was 3.17 (2.67, 3.67) dB.

All study methods were approved by the University of California San Diego Human Research Protection Program and adhered to the provisions of the Declaration of Helsinki guidelines for research involving human participants and the Health Insurance Portability and Accountability Act (HIPAA).

### PERG

A commercially available modification of the Glaid (software version 2.1.14, Lace Elettronica) electrophysiology instrument, called PERGLA, was used to measure the PERG response.<sup>20,21</sup> Stimulus and recording parameters were determined by the PERGLA paradigm. The stimulus was a black and white (contrast 98%, mean luminance 40 cd/m<sup>2</sup>), horizontal square wave grating (1.6 c/degree), counter phasing at 8.14 Hz, presented on a computer monitor (14.1 cm diameter circular field). At a viewing distance of 30 cm, the display subtended 25 degrees centred on the fovea. Responses from both eyes were measured simultaneously. Electrical signals from silver–chloride skin electrodes (adhered

with conductive cream and tape; both lower eyelids active, both temples reference, forehead ground) were fed into a two-channel differential amplifier, amplified (100 000-fold), filtered (1–30 Hz), and then digitized with 12-bit resolution at 4169 Hz. Before testing, electrode impedance was monitored automatically and an on-screen indicator assured acceptable impedance ( $\leq 5 \text{ k}\Omega$ ). Additionally, pre-test background noise was monitored by viewing an on-screen oscilloscope.

Each steady-state waveform was obtained by averaging 600 artifact-free time periods (sweeps) of 122.8 ms each, synchronized with the contrast alternation of the stimulus grating. Two independent response blocks of 330 sweeps each were recorded and separated by a user-defined interval ( $\sim 1$  min). For each block, the first 30 sweeps were rejected from the average to eliminate onset effects from the steady-state recording. Sweeps containing spurious signals attributable to blinks and eye movements were rejected over a threshold voltage of  $\pm 25 \mu\text{V}$ . Resulting steady-state PERGs were in the form of near-sine waves that were Fourier transformed to isolate the harmonic component at the contrast reversal rate (16.28 Hz, two contrast reversals per cycle). In addition, a noise response was obtained by multiplying alternate sweeps by 1 and  $-1$  before averaging. The noise response was also Fourier transformed at 16.28 Hz to allow calculation of SNR. Reported reproducibility of PERGLA measurements is excellent.<sup>20,22–24</sup>

The same operator (AT) tested each participant. All eyes were refracted, appropriate corrections for viewing distance were made, and near acuity was J1 or better.<sup>21,25</sup> The average (95% CI) signal-to-noise ratio of all PERG amplitude measurements was  $4.21 \mu\text{V}$  ( $3.56 \mu\text{V}$ ,  $4.86 \mu\text{V}$ ).

### SD-OCT

SD-OCT imaging was obtained using the RTVue 100 (software version 2.0.4.0, Optovue Inc.). Similar to time domain-OCT (TD-OCT), SD-OCT measurements are obtained by comparing the time delay of light reflected from a tissue sample to a known reference standard (ie, interference). SD-OCT uses a stationary rather than a movable reference mirror allowing axial scans (A-scans) to be obtained as an array rather than individually. The interference between the sample and reference reflections is split into a spectrum and captured by a line camera. The spectral interferogram is then Fourier transformed to provide thickness measurements of the entire A-scan array. The RTVue uses a scanning laser diode to emit a scan beam of wavelength =  $840 \pm 10 \text{ nm}$ . The image acquisition rate is 26 000 A-scans per second. Axial resolution is  $4 \mu\text{m}$  with a beam spot size of  $15 \mu\text{m}$ , and the scan range is 2.0–2.3 mm in the z-direction and

2.0–12.0 mm in the xy-directions. Reported reproducibility of RTVue measurements is excellent.<sup>26</sup>

In this study, the 3D, GCC, and NHM4 RTVue SD-OCT protocols were used. The 3D protocol provided an *en-face* image on which to draw the contour line describing the disc margin required to generate RNFL and optic disc parameters from the NHM4 protocol (below). This scan is a  $4 \times 4 \text{ mm}$  raster scan centred on the optic disc and composed of 101 B-scans, each composed of 512 A-scans (acquisition time = 2.2 s). The resulting scan provides a 3D image of the optic disc and parapapillary area. The contour line was initially drawn on the *en-face* image by hand. The position of the contour line was then assessed, and if necessary, corrected by examining the interface between its position and the position of the retinal pigment epithelium (RPE) tips in approximately eight locations.

Macular thickness was measured using the GCC protocol. This protocol is composed of 15 vertically oriented B-scans of 7.0 mm in length (800 A-scans each), each separated by 0.50 mm and a single horizontally oriented B-scan of 7.0 mm in length (12 934 A-scans), all centred (roughly) on the macula by the operator (the center of the GCC scan is shifted 1.0 mm temporally to better sample the temporal peripheral macula that is associated with the nasal visual field). This scan configuration provides a total of 24 934 A-scans in 1.0 s. Areas between A-scans are interpolated.

Macular thickness measurements reported are GCC thickness (software-defined region bound by the presumed internal-limiting membrane and inner plexiform layers), macular thickness (software-defined region bound by the presumed internal-limiting membrane and bottom of the RPE), and macular outer retinal thickness (defined as macular thickness minus GCC thickness).

RNFL thickness and optic disc topography were measured using the NHM4 protocol. This protocol is composed of 12 radial scans of 3.4 mm in length (452 A-scans each) and 6 concentric ring scans ranging from 2.5 to 4.0 mm diameter (587 or 775 A-scans each), all centred on the optic disc (using the previously drawn contour line to ensure scan registration). This scan configuration provides 9510 total A-scans in 0.39 s. Areas between A-scans are interpolated. A polar RNFL thickness map and various parameters that describe the optic disc topography (see below) are provided. RNFL thickness measurements are obtained for the 3.45 mm radius ring only.

The RNFL measurement reported is average RNFL thickness (based on 360 degree measurement). RNFL thickness is measured by assessing 2325 data points between the anterior and posterior RNFL borders. Optic disc measurements reported from the NHM4 protocol

are rim area and rim volume. To determine these measurements, the outer optic disc margin is defined by the RPE tip-based contour line, and the neuroretinal rim and optic cup are defined relative to a surface 150  $\mu\text{m}$  above the plane connecting the RPE tips. The average (95% CI) signal strength of all SD-OCT GCC measurements was 61.99 (60.49, 63.48) with minimum signal strength of 45.55, and the average (95% CI) signal strength of all NMH4 measurements was 57.05 (55.61, 58.50) with minimum signal strength of 37.09.

### Analyses

Associations were investigated using regression (with linear mixed models using restricted maximum likelihood to control for inter-eye dependence) between PERG amplitude and SD-OCT macular thickness, RNFL thickness and optic disc topography measurements, all expressed in linear units. Results are reported as  $R^2$ .

To determine whether PERG amplitude was more strongly associated with any structural measurement, the absolute value of the studentized residuals from each regression model were log transformed (because absolute value of the residuals were not normally distributed) and compared by repeated measures ANOVA with pairwise Tukey *post-hoc* comparisons.<sup>27,28</sup> Studentized residuals were used because they are scale free (they represent the residuals in SD form) and the measurement scales are different across parameters investigated in the current study (eg,  $\mu\text{V}$  PERG amplitude,  $\mu\text{m}$  RNFL and macular thickness,  $\text{mm}^2$  neuroretinal rim area, and  $\text{mm}^3$  neuroretinal rim volume).

### Results

Demographic, functional, and structural measurements are shown in Table 1. Associations between PERG amplitude and SD-OCT measurements are shown in Table 2. PERG amplitude was most strongly associated with GCC thickness ( $R^2 = 0.179$ ,  $P < 0.001$ ), followed by RNFL thickness ( $R^2 = 0.174$ ,  $P < 0.001$ ), and macular thickness ( $R^2 = 0.095$ ,  $P < 0.001$ ). All significant associations were in the expected direction, with PERG amplitude decreasing with decreases in tissue thickness. Associations with other parameters were not significant (all  $P \geq 0.624$ ). Significant associations remained for GCC ( $P = 0.021$ ) and average RNFL thickness ( $P = 0.030$ ), but not for macular thickness, when participant age and IOP at the time of testing were included in multivariable models. Figure 1 shows graphically the statistically significant linear univariate associations between PERG and SD-OCT measurements.

**Table 1** Demographic, functional, and structural measurements

Parameter (unit of measure)	Mean (95% CI) (n = 132 eyes of 66 participants)
Age (years)	67.9 (65.8, 70.0)
Gender (percent female)	54
Race (percent Caucasian)	88
SAP MD (dB)	-1.92 (-2.45, -1.39)
SAP PSD (dB)	3.17 (2.67, 3.67)
IOP (mm Hg)	15.8 (14.9, 16.6)
PERG amplitude ( $\mu\text{V}$ )	0.58 (0.54, 0.62)
SD-OCT GCC thickness ( $\mu\text{m}$ )	86.7 (85.1, 88.3)
SD-OCT macular thickness ( $\mu\text{m}$ )	259.7 (257.3, 262.1)
SD-OCT macular outer retinal thickness ( $\mu\text{m}$ )	173.0 (171.3, 174.6)
SD-OCT RNFL thickness ( $\mu\text{m}$ )	90.9 (88.8, 92.9)
SD-OCT rim area ( $\text{mm}^2$ )	0.98 (0.92, 1.04)
SD-OCT rim volume ( $\text{mm}^3$ )	0.17 (0.14, 0.19)

Abbreviations: CI, confidence interval; GCC, ganglion cell complex; IOP, intraocular pressure; MD, mean deviation; PERG, pattern electroretinogram; PSD, pattern SD; SAP, standard automated perimetry; RNFL, retinal nerve fibre layer; SD-OCT, spectral domain-optical coherence tomography.

**Table 2** Associations ( $R^2$ ) between PERG amplitude and SD-OCT structural measurements

Parameter	$R^2$	P-value
SD-OCT GCC thickness	0.179	<0.0001
SD-OCT macular thickness	0.095	<0.0001
SD-OCT macular outer retinal thickness	0.003	0.934
SD-OCT RNFL thickness	0.174	<0.0001
SD-OCT rim area	0.007	0.823
SD-OCT rim volume	0.014	0.624

Abbreviations: GCC, ganglion cell complex; PERG, pattern electroretinogram; RNFL, retinal nerve fibre layer; SD-OCT, spectral domain-optical coherence tomography.

The associations between PERG amplitude and GCC thickness, RNFL thickness and macular thickness were similar (all Tukey pairwise comparisons between these associations,  $P \geq 0.05$ ) and were statistically greater than the associations between PERG amplitude and macular outer retinal thickness, rim volume and rim area (all Tukey pairwise comparisons between these associations and the associations described above,  $P \leq 0.030$ ). A subset analysis, including measurements from glaucoma patients only (glaucoma suspects omitted), showed very similar results.  $R^2$  associations differed by a minimum of 0.001 greater (for outer retinal thickness,  $R^2 = 0.004$  compared with  $R^2 = 0.003$ ) to a maximum of 0.019 greater (for GCC thickness  $R^2 = 0.198$  compared to  $R^2 = 0.174$ ). The resulting associations were not significantly different from the associations observed for the total patient population.

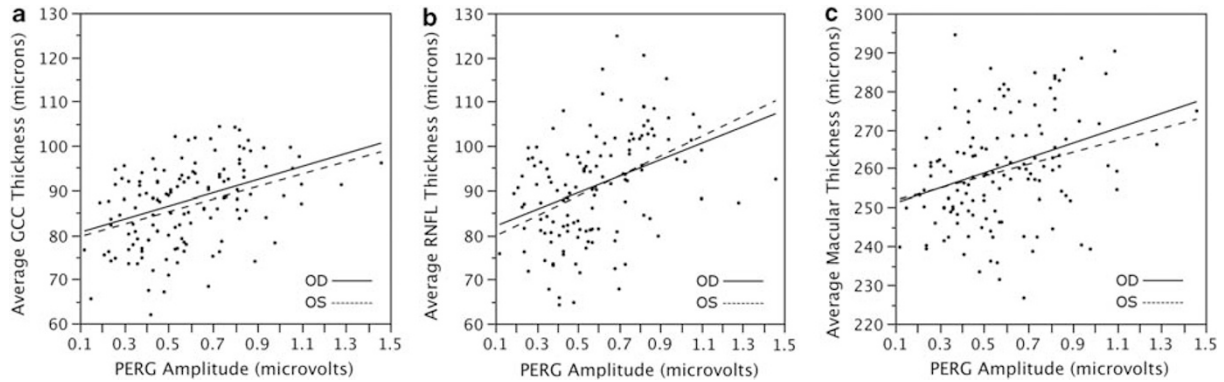


**Figure 1** Scatterplots showing the significant associations between PERG amplitude and SD-OCT-measured (a) macular GCC thickness ( $R^2=0.179$ ,  $P<0.001$ ), (b) RNFL thickness ( $R^2=0.174$ ,  $P<0.001$ ), and (c) macular thickness ( $R^2=0.095$ ,  $P<0.001$ ). Associations with other parameters were not statistically significant and data are not shown.

Figure 2 shows subjectively defined examples of agreement and disagreement between PERG and SD-OCT measurements. In panel a, PERG amplitude is low ( $0.38 \mu V$ , outside of normal limits by the PERGLA normative database<sup>20</sup>) and both GCC and RNFL measurements indicate below average tissue thickness. Optic disc topography parameters are borderline compared with normative data. SAP MD for this patient is  $-2.92$  dB with PSD and GHT outside of normal limits. The participant was 69.4 years old, and IOP was 15 mmHg at the time of testing. In panel b, PERG amplitude is high ( $0.82 \mu V$  and within normal limits) and GCC, RNFL, and optic disc topography measurements all are within normal limits. SAP MD is  $-0.40$  dB and global indices are within normal limits. The participant was 49.2 years old, and IOP was 15 mmHg. Next, in panel c, PERG amplitude is very low ( $0.26 \mu V$ , outside normal limits), whereas SD-OCT measurements are generally within the normal range and SAP MD is  $-0.36$  dB and within normal limits, possibly suggesting ganglion cell dysfunction preceding cell death. This participant was 67.8 years old, and IOP was 14 mmHg. Finally, in panel d, PERG amplitude is high ( $0.73 \mu V$ ), whereas SD-OCT GCC and RNFL measurements are very low. SAP MD is  $-0.65$  dB and within normal limits, possibly suggesting structural defects preceding retinal function and visual field disturbances. The participant was 64.2 years old, and IOP was 17 mmHg. For the two cases of disagreement, longitudinal follow-up is required to confirm or disprove the disease-stage scenarios suggested. The apparent disagreement between functional and structural measurements illustrated in this Figure (and to some degree in Figure 1) suggests that, although associations between PERG and SD-OCT measurements exist on a population level, caution

should be used when expecting these associations in all individual cases.

### Discussion

The current study describes the low/moderate to statistically non-significant associations between PERG amplitude and SD-OCT measurements of macular thickness, RNFL thickness and optic disc topography. The strengths of associations generally were similar to those described previously using TD-OCT, SLP, and CSLO.<sup>9</sup>

We found the strongest association between PERG amplitude and GCC thickness (although this association was not significantly stronger than all others), and a much weaker association between PERG amplitude and outer macular thickness (ie, retinal structures presumed not responsible for the PERG response). These results add *in vivo* anatomical support to the idea that the PERG response is primarily representative of retinal ganglion cell function as opposed to a response of all retinal cells that contribute to visual function (see<sup>29</sup> for a review of the cellular origins of the PERG). The significant associations between PERG amplitude and average RNFL thickness in our study and others support the idea that PERG is measuring more than a central response.<sup>30,24</sup>

The observed lack of association between centrally measured PERG amplitude and optic disc topography might be because, in part, of the relatively small contribution of the temporal rim area (region most closely associated with central vision) to global rim area measurements recorded in our study. In fact, others have reported significant associations between PERG measurements and sectoral topography measurements. For instance, Salgarello *et al*<sup>10</sup> found a significant negative (ie, in the expected direction) association ( $r = -0.43$ )

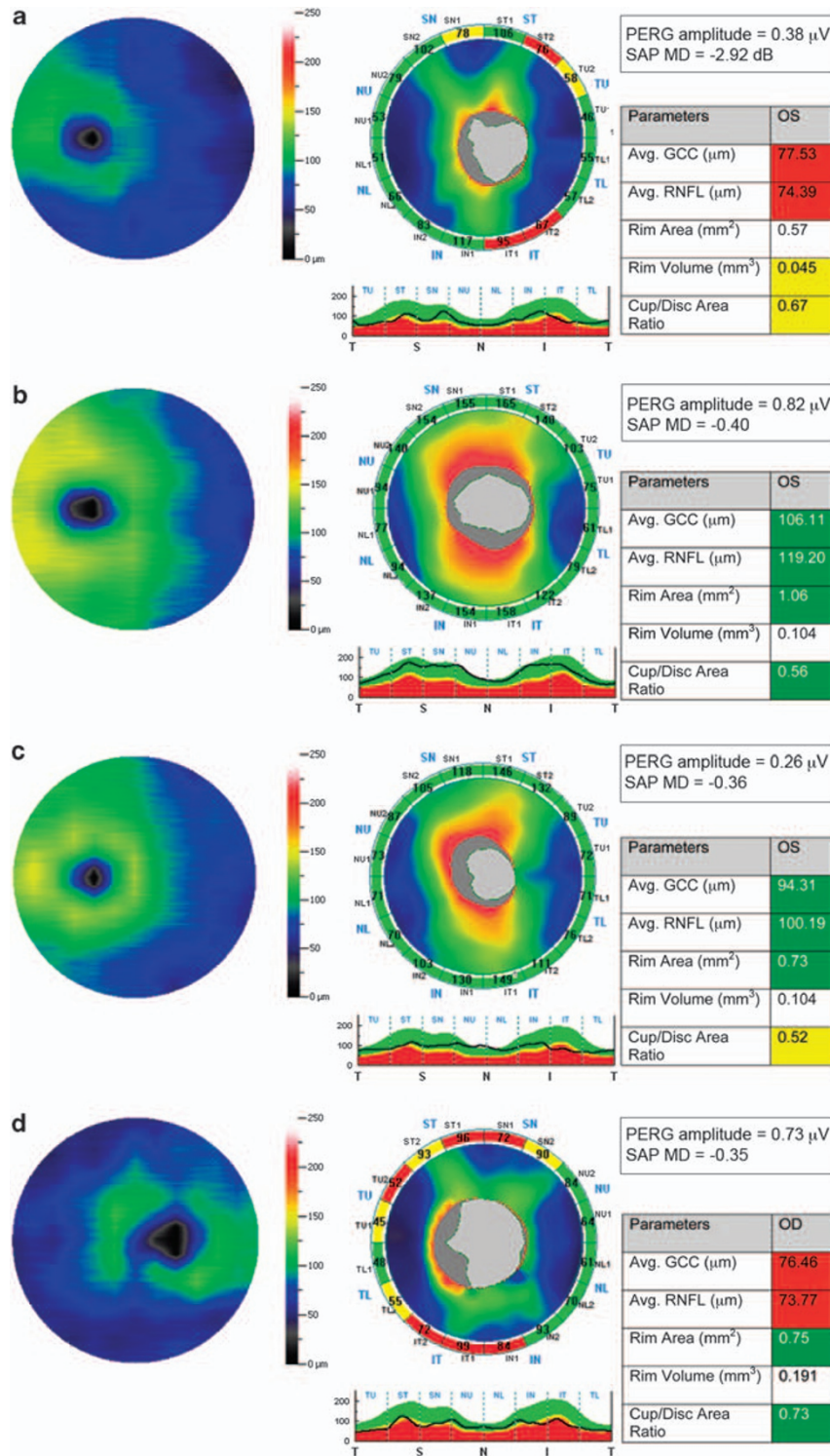


**Figure 2** Case examples showing subjectively defined agreement (a, b) and disagreement (c, d) between PERG amplitude and SD-OCT measurements. Each panel shows (from left to right) SD-OCT macular GCC thickness maps, retinal nerve RNFL thickness maps, and parameter measurements with corresponding normative database results. In panel a, representing agreement, PERG amplitude is low (0.38  $\mu$ V) and both GCC and RNFL measurements indicate below average tissue thickness. In panel b, also representing agreement, PERG amplitude is high (0.82  $\mu$ V) and both GCC and RNFL measurements indicate tissue thickness within normal limits. In panel c, representing disagreement, PERG amplitude is low (0.26  $\mu$ V) and both GCC and RNFL measurements indicate tissue thickness within normal limits. In panel d, representing disagreement, PERG amplitude is high (0.73  $\mu$ V) and both GCC and RNFL measurements indicate below average tissue thickness. See text for more details.

between PERG amplitude and inferior temporal CSLO-measured cup shape in ocular hypertensive (OHT) eyes, whereas associations with other CSLO parameters were not significant. Further, Garway-Heath *et al*<sup>8</sup> found significant associations between steady-state and transient PERG amplitude and temporal CSLO-measured rim area ( $R^2 = 0.20$  and  $0.17$ , respectively).

Recently, Sehi *et al*<sup>9</sup> investigated the association between PERG amplitude, using the PERGLA paradigm, and global rim area measured using CSLO, and found no significant association in glaucoma or glaucoma suspect eyes, similar to the current study. Moreover, these authors found moderate associations in glaucoma eyes that were slightly stronger than associations reported in the current study between PERGLA amplitude and global (and regional) RNFL thickness measured using both TD-OCT and SLP. Average SAP MD in the former study was  $-5.01$  dB compared with  $-1.92$  dB in our study. This difference in glaucoma severity may have contributed to the slightly different results. Sehi *et al*<sup>9</sup> did not find significant structure–function associations in glaucoma suspect eyes, possibly because many of their suspect eyes likely were OHT (evidenced by an average SAP MD similar to that in their normal group; average SAP MD =  $-0.30$  and  $-0.20$  dB, respectively) with a restricted range of structural measurements.

Also using the PERGLA paradigm and StratusOCT (Carl Zeiss Meditec, Dublin, CA, USA), Ventura *et al*<sup>12</sup> reported structure–function associations that were stronger in glaucoma suspect eyes (observable disc damage with SAP results within normal limits, average SAP MD =  $-0.58$  dB) than in eyes with early glaucoma (observable disc damage with repeatable SAP results outside normal limits, average SAP MD =  $-2.70$  dB). Associations were  $r = 0.31$  and  $r = 0.17$  (not statistically significant), respectively. It is not clear why significant associations were found in glaucoma eyes only in one study and suspect eyes only in the other. However, that the latter study used age-corrected values of PERG amplitude and RNFL thickness, whereas the former did not may have contributed to this difference. Also, it is possible that differing IOP among groups in the different studies was a contributing factor. Although IOP is not reported in either study, in the latter study, a higher percentage of glaucoma eyes than suspect eyes were treated with IOP-lowering medications. Therefore, stronger associations in suspect eyes could be partially the result of reduced PERG amplitude caused by untreated IOP in the presence of early structural damage. Finally, it is possible that the differing results exist because the compared features are weakly correlated, in general.

Other studies have described the structure–function association using both steady-state and transient PERG with varying results. For instance, Bach and Funk<sup>14</sup>

showed no correlation between PERG index (age-corrected linear combination of steady-state PERG amplitudes generated using 0.8 and 19 degree checks) and rim area or disc area measured using an early CSLO in OHT eyes, whereas Salgarello *et al*<sup>10</sup> and Garway-Heath *et al*<sup>8</sup> did find an association using PERG amplitude and disc topography measured using the more recent HRT (as described above).

Using TD-OCT (pre-StratusOCT), Parisi *et al* described significant correlations between transient PERG measurements and RNFL thickness obtained in all quadrants, except the nasal quadrant in OHT eyes.<sup>13</sup> For PERG P50 minus N95 amplitude,  $r$  ranged from  $0.181$  ( $P = 0.321$ ) nasally to  $0.606$  ( $P < 0.001$ ) superiorly. Additionally, strong associations were observed between PERG P50 implicit time and global ( $r = -0.847$ ) and temporal ( $r = -0.823$ ) RNFL thickness in somewhat advanced glaucoma eyes (average SAP MD approximately  $-12.40$  dB).<sup>11</sup> More recently, Falsini *et al* described associations between steady-state PERG amplitude and StratusOCT-measured average, superior and inferior RNFL thickness ( $r$  ranged from  $0.33$  to  $0.47$ ) in early glaucoma (average MD =  $-2.5$  dB).<sup>17</sup>

Based on our results and those of others, associations between PERG amplitude and structure measured using optical imaging in early glaucoma are variable at best and tentative at worst. This may be because, in part, of the reported association between PERG amplitude and IOP<sup>20</sup> and the reported sensitivity of the PERG response to changes in IOP.<sup>30,31</sup> The relationship between the PERG and changes in IOP appears to be complex in that PERG changes resulting from changes in IOP may occur only in eyes that have PERG deficits in the first place and may occur only in early glaucoma.<sup>30</sup> These complexities might help explain the disparate structure–function results observed when using PERG (see<sup>32–34</sup> for other possibilities). For instance, PERG amplitude in treated patients may not accurately represent the true disease state because induced decreases in IOP may result in concomitant increases in amplitude. Sensitivity to IOP suggests that the PERG may be sensitive to intermittent cell dysfunction in addition to cell death, whereas retinal thickness/topography should not be sensitive to such dysfunction. In general, it is important for physicians who use PERG clinically to understand the association between the PERG response and the underlying structural condition. However, these associations likely are too complex and variable to be used to assess strictly the effect of ganglion cell count on visual sensitivity or as a basis for developing theories about the relative time course of glaucomatous structural and functional change.

The most important findings from the current study are the relative strengths of association between PERG amplitude and different retinal structures measured in

the same eyes using the same instrument. Because of its high resolution, it is assumed that SD-OCT currently is the ideal surrogate for direct tissue measurement. However, the accuracy of SD-OCT for identifying retinal structures may be more dependant on tissue segmentation algorithms than that on image resolution, and improvements in segmentation algorithms (and changes in sampling pattern densities) may influence the results of future SD-OCT-based investigations of the structure–function relationship in glaucoma.

Overall, results from this study indicate that PERG amplitude, as an assumed indicator of retinal ganglion cell activity, is significantly associated with macular GCC thickness, as an assumed indicator of retinal ganglion cell count. Although only low to moderate in strength, this association was significantly greater than the non-significant association between PERG amplitude and outer retinal thickness, and considerably greater than its association with overall macular thickness. In addition, results were significant in a multivariate model that included IOP and age at the time of testing. These results suggest that the PERG response provides a reasonable functional assessment of retinal ganglion cell count.

### Summary

#### What was known before

- Associations between PERG amplitude and optic disc and RNFL topographic measurements in glaucoma eyes are reportedly weak to moderate, as measured using earlier generation optical imaging instruments.

#### What this study adds

- Significant but weak associations were found between PERG amplitude and SD-OCT-measured macular GCC thickness, RNFL thickness and macular thickness. Associations with disc topography were not significant.

### Conflict of interest

Carl Zeiss Meditec: LMZ (F), FAM (C, F, L), PAS (F), and RNW (C, F); Heidelberg Engineering: LMZ (F) and RNW (C, F); Luce Eletttronica: CB (F); and Optovue: LMZ (F) and RNW (C).

### Acknowledgements

This study was supported by NIH EY018190, NIH EY008208, and participant incentive grants in the form of glaucoma medication at no cost from Alcon Laboratories Inc., Allergan, Pfizer Inc., Merck & Co. Inc., and Santen Inc.

### References

1 Maffei L, Fiorentini A. Electroretinographic responses to alternating gratings before and after section of the optic nerve. *Science* 1981; **211**(4485): 953–955.

2 Maffei L, Fiorentini A, Bisti S, Hollander H. Pattern ERG in the monkey after section of the optic nerve. *Exp Brain Res* 1985; **59**(2): 423–425.

3 Baker Jr CL, Hess RR, Olsen BT, Zrenner E. Current source density analysis of linear and non-linear components of the primate electroretinogram. *J Physiol* 1988; **407**: 155–176.

4 Hood DC, Frishman LJ, Viswanathan S, Robson JG, Ahmed J. Evidence for a ganglion cell contribution to the primate electroretinogram (ERG): effects of TTX on the multifocal ERG in macaque. *Vis Neurosci* 1999; **16**(3): 411–416.

5 Parisi V. Neural conduction in the visual pathways in ocular hypertension and glaucoma. *Graefes Arch Clin Exp Ophthalmol* 1997; **235**(3): 136–142.

6 Weinreb RN, Khaw PT. Primary open-angle glaucoma. *Lancet* 2004; **363**(9422): 1711–1720.

7 Trick GL. The pattern electroretinogram in glaucoma and ocular hypertension. In: Heckenlively JR, Arden GB (eds). *Principles and Practice of Clinical Electrophysiology of Vision*. The MIT Press: Cambridge, MA, 2006.

8 Garway-Heath DF, Holder GE, Fitzke FW, Hitchings RA. Relationship between electrophysiological, psychophysical, and anatomical measurements in glaucoma. *Invest Ophthalmol Vis Sci* 2002; **43**(7): 2213–2220.

9 Sehi M, Pinzon-Plazas M, Feuer WJ, Greenfield DS. Relationship between pattern electroretinogram, standard automated perimetry, and optic nerve structural assessments. *J Glaucoma* 2009; **18**(8): 608–617.

10 Salgarello T, Colotto A, Falsini B, Buzzonetti L, Cesari L, Iarossi G *et al*. Correlation of pattern electroretinogram with optic disc cup shape in ocular hypertension. *Invest Ophthalmol Vis Sci* 1999; **40**(9): 1989–1997.

11 Parisi V, Manni G, Centofanti M, Gandolfi SA, Olzi D, Bucci MG. Correlation between optical coherence tomography, pattern electroretinogram, and visual evoked potentials in open-angle glaucoma patients. *Ophthalmology* 2001; **108**(5): 905–912.

12 Ventura LM, Sorokac N, De Los Santos R, Feuer WJ, Porciatti V. The relationship between retinal ganglion cell function and retinal nerve fiber thickness in early glaucoma. *Invest Ophthalmol Vis Sci* 2006; **47**(9): 3904–3911.

13 Parisi V, Manni G, Gandolfi SA, Centofanti M, Colacino G, Bucci MG. Visual function correlates with nerve fiber layer thickness in eyes affected by ocular hypertension. *Invest Ophthalmol Vis Sci* 1999; **40**(8): 1828–1833.

14 Bach M, Funk J. Pattern electroretinogram and computerized optic nerve-head analysis in glaucoma suspects. *Ger J Ophthalmol* 1993; **2**(3): 178–181.

15 Bomer TG, Meyer JH, Bach M, Funk J. Pattern electroretinogram and computerized optic nerve-head analysis in ocular hypertension—interim results after 2.5 years. *Ger J Ophthalmol* 1996; **5**(1): 26–30.

16 Parisi V. Correlation between morphological and functional retinal impairment in patients affected by ocular hypertension, glaucoma, demyelinating optic neuritis and Alzheimer’s disease. *Semin Ophthalmol* 2003; **18**(2): 50–57.

17 Falsini B, Marangoni D, Salgarello T, Stifano G, Montrone L, Campagna F *et al*. Structure-function relationship in ocular hypertension and glaucoma: interindividual and interocular analysis by OCT and pattern ERG. *Graefes Arch Clin Exp Ophthalmol* 2008; **246**(8): 1153–1162.

18 Caprioli J, Miller JM. Correlation of structure and function in glaucoma. Quantitative measurements of disc and field. *Ophthalmology* 1988; **95**(6): 723–727.

19 Anderson DR, Patella VM. *Automated Static Perimetry*, 2nd edn. Mosby: St Louis, MO, 1998.



- 20 Porciatti V, Ventura LM. Normative data for a user-friendly paradigm for pattern electroretinogram recording. *Ophthalmology* 2004; **111**(1): 161–168.
- 21 Ventura LM, Porciatti V, Ishida K, Feuer WJ, Parrish II RK. Pattern electroretinogram abnormality and glaucoma. *Ophthalmology* 2005; **112**(1): 10–19.
- 22 Bowd C, Tafreshi A, Vizzeri G, Zangwill LM, Sample PA, Weinreb RN. Repeatability of pattern electroretinogram measurements using a new paradigm optimized for glaucoma detection. *J Glaucoma* 2009; **18**(6): 437–442.
- 23 Fredette MJ, Anderson DR, Porciatti V, Feuer W. Reproducibility of pattern electroretinogram in glaucoma patients with a range of severity of disease with the new glaucoma paradigm. *Ophthalmology* 2008; **115**(6): 957–963.
- 24 Yang A, Swanson WH. A new pattern electroretinogram paradigm evaluated in terms of user friendliness and agreement with perimetry. *Ophthalmology* 2007; **114**(4): 671–679.
- 25 Vizzeri G, Tafreshi A, Weinreb RN, Bowd C. Effect of operator and optical defocus on the variability of pattern electroretinogram optimized for glaucoma detection (PERGLA). *J Glaucoma* 2010; **19**(2): 77–82.
- 26 Gonzalez-Garcia AO, Vizzeri G, Bowd C, Medeiros FA, Zangwill LM, Weinreb RN. Reproducibility of RTVue retinal nerve fiber layer thickness and optic disc measurements and agreement with Stratus optical coherence tomography measurements. *Am J Ophthalmol* 2009; **147**(6): 1067–1074.
- 27 Bowd C, Zangwill LM, Medeiros FA, Tavares IM, Hoffmann EM, Bourne RR *et al*. Structure-function relationships using confocal scanning laser ophthalmoscopy, optical coherence tomography, and scanning laser polarimetry. *Invest Ophthalmol Vis Sci* 2006; **47**(7): 2889–2895.
- 28 Bowd C, Tavares IM, Medeiros FA, Zangwill LM, Sample PA, Weinreb RN. Retinal nerve fiber layer thickness and visual sensitivity using scanning laser polarimetry with variable and enhanced corneal compensation. *Ophthalmology* 2007; **114**(7): 1259–1265.
- 29 Bach M, Hoffmann MB. The origin of the pattern electroretinogram. In: Heckenlively JR, Arden GB (eds). *Principles and Practice of Clinical Electrophysiology of Vision*, 2nd edn. MIT Press: Cambridge, MA, 2006.
- 30 Ventura LM, Porciatti V. Restoration of retinal ganglion cell function in early glaucoma after intraocular pressure reduction: a pilot study. *Ophthalmology* 2005; **112**(1): 20–27.
- 31 Kremmer S, Tolksdorf-Kremmer A, Stodtmeister R. (Simultaneous registration of VECP and pattern ERG during artificially raised intraocular pressure). *Ophthalmologica* 1995; **209**(5): 233–241.
- 32 Bach M, Schumacher M. The influence of ambient room lighting on the pattern electroretinogram (PERG). *Doc Ophthalmol* 2002; **105**(3): 281–289.
- 33 Otto T, Bach M. Retest variability and diurnal effects in the pattern electroretinogram. *Doc Ophthalmol* 1996; **92**(4): 311–323.
- 34 Porciatti V, Sorokac N, Buchser W. Habituation of retinal ganglion cell activity in response to steady state pattern visual stimuli in normal subjects. *Invest Ophthalmol Vis Sci* 2005; **46**(4): 1296–1302.